



Solar radiation regulates the leaf nitrogen and phosphorus stoichiometry across alpine meadows of the Tibetan Plateau



Jian Sun^{a,b,c,*}, Biying Liu^d, Yong You^e, Weipeng Li^e, Miao Liu^a, Hua Shang^c, Jin-Sheng He^f

^a Synthesis Research Centre of Chinese Ecosystem Research Network, Key Laboratory of Ecosystem Network Observation and Modelling, Institute of Geographic Sciences and Natural Resources Research, Chinese Academy of Sciences, Beijing, 100101, China

^b State Key Laboratory of Urban and Regional Ecology, Research Center for Eco-Environmental Sciences, Chinese Academy of Sciences, Beijing, 100085, China

^c Department of Ecology, Evolution, and Natural Resources, School of Environmental and Biological Sciences, Rutgers University, New Brunswick, NJ, 08901, USA

^d College of Earth Sciences, Chengdu University of Technology, Chengdu, 610059, China

^e Land and Resources College, China West Normal University, Nanchong, 637009, China

^f State Key Laboratory of Grassland Agro-ecosystems, and College of Pastoral, Agriculture Science and Technology, Lanzhou University, China

ARTICLE INFO

Keywords:

Solar radiation
Leaf stoichiometry
Nitrogen
Phosphorus
Alpine meadow
Tibetan Plateau

ABSTRACT

Leaf nitrogen (N) and phosphorus (P) stoichiometry covary with many aspects of climatic and edaphic factors, yet the effects of solar radiation (SR) on leaf stoichiometry are still unclear. In the Tibetan Plateau, the high level of SR can induce the plants to reach their light saturation point easily, which causes photoinhibition of photosynthesis. Here, the leaf N and P concentrations across the alpine meadow of the Tibetan Plateau were measured to explore the response of leaf N and P stoichiometry to SR. Our results showed that the concentrations of both leaf N and leaf P were negatively correlated with SR under the high SR level ($SR > 15,000 \text{ KJ m}^{-2} \text{ d}^{-1}$). The structural equation model demonstrated that SR plays a vital role in leaf N and P stoichiometry, and SR has direct effects on leaf N and P stoichiometry through a physiological process (path coefficient = -0.293 and -0.343, respectively). In addition, the high SR level lowered the level of precipitation (path coefficient = -0.615) and temperature (path coefficient = -0.047), then changed the soil organic carbon, soil nitrogen and phosphorus content. Furthermore, precipitation, temperature, soil organic carbon, soil nitrogen and phosphorus also regulated leaf N and P stoichiometry, which caused the SR to have indirect effects on leaf N and P stoichiometry (path coefficient = -0.072 and -0.053, respectively). As a consequence, we highlighted that SR regulates leaf N and P stoichiometry across alpine meadows of the Tibetan Plateau, and the results provide guidance on grassland management.

1. Introduction

Nitrogen and phosphorus play critical roles in controlling ecosystem functions and services, which are generally considered to be the most limiting elements to the terrestrial ecosystem (Reich and Oleksyn, 2004). Ecological stoichiometry, especially leaf N and P stoichiometry, has attracted increasing attention (Wu et al., 2012) recently. Previous studies have explored the dynamics of plant leaf N and P stoichiometry at regional, national and global scales (Han et al., 2005; He et al., 2008; Reich and Oleksyn, 2004). Generally, the results demonstrated that leaf N and P concentrations and the N:P ratio are regulated by biotic and abiotic factors (Güsewell, 2004), especially the plant functional traits (Li et al., 2010), edaphic variables (Hobbie and Gough, 2002), and

geographic and climatic features (Chen et al., 2013). For plant functional traits, some studies have indicated that leaf N concentration is controlled by the influence of the specific leaf area on photosynthesis (Reich et al., 1998) and the relative growth rate (Vanni et al., 2002); other research has reported that leaf dry matter content has a significant correlation with the leaf P concentration and the leaf N:P ratio (Wu et al., 2012). In addition, the leaf stoichiometry varies in individual genus/species levels (Kang et al., 2011; Li et al., 2010). Moreover, the soil properties determine the plant survival strategy and adaptation in alpine ecosystems (Sun et al., 2018; Sun and Wang, 2016b; Sun et al., 2014). For example, plant leaf N and P concentrations are mainly governed by soil nutrients (soil N and P concentrations) and different species in tundra (Hobbie and Gough, 2002). For geographic

* Corresponding author at: Institute of Geographic Sciences and Natural Resources Research, Chinese Academy of Sciences (CAS), 11 A, Datun Road, Chaoyang District, Beijing, 100101, China.

E-mail addresses: sunjian@igsnr.ac.cn (J. Sun), lby362428@163.com (B. Liu), Youy9689@163.com (Y. You), wpliwenli@163.com (W. Li), liumiao@igsnr.ac.cn (M. Liu), hua.shang@rutgers.edu (H. Shang), jshe@pku.edu.cn (J.-S. He).

<https://doi.org/10.1016/j.agrformet.2019.02.041>

Received 20 August 2018; Received in revised form 28 January 2019; Accepted 28 February 2019

0168-1923/ © 2019 Elsevier B.V. All rights reserved.

and climatic factors, existing publications discovered that the leaf N:P ratio increased with increasing longitude (Wu et al., 2014), while the leaf N:P ratio was negatively related to latitude (Hedin, 2004). Additionally, leaf stoichiometry was strongly correlated to the mean annual precipitation and mean annual evaporation for global flora (Ordoñez et al., 2009). In fact, the response of plant functional traits is mediated by the interactions of geographic and climatic features and soil properties (Noymeir, 1973; Sun et al., 2013b). For instance, the increased net primary productivity with the increasing longitude from west to east in China leads to a gradual increase in the soil organic matter and soil N content (Ni et al., 2001), and the increase of precipitation exacerbates the loss of nutrients from leaf and soil (Esmeijer-Liu et al., 2009), which directly induces a decline in leaf P concentration (Manzoni et al., 2010).

As a climatic factor, solar radiation (SR) plays a vital role in the accumulation of leaf N and P. For example, for leaf N, 71% of the climatic factors exist in combination with proteins (Takashima and Hikosaka, 2010), while the process of photosynthesis, net ecosystem exchange, and the synthesis of proteins, sugars and acids were all significantly influenced by SR (Goulden et al., 1997; Zhang et al., 2009). Zheng et al. (2012b) indicated the same result for leaf P; the decrease of SR leads to an increase in the transit of leaf P and results in the distribution rate of leaf P increasing remarkably. On the other hand, light, soil nutrients, precipitation and temperature, which are influenced by the SR, also change the distribution of leaf N and P (Ren et al., 2003). Nevertheless, the responding mechanisms of plant leaf N and P stoichiometry to a high SR region, like the Tibetan Plateau, are still unclear, and there is no full account of the interaction among SR, precipitation, temperature, soil factors and plant leaf N and P stoichiometry. Thus, we hypothesize that SR is a vital factor that directly affects the leaf N and P stoichiometry via physiological processes, and SR also regulates the leaf N and P stoichiometry indirectly via climatic (Law et al., 2002) and edaphic (Duan and Guo, 1992) variables (Fig. 1).

The area of the Tibetan Plateau, which is the highest plateau in the world, is dominated by an approximately 35% alpine meadow ecosystem (Sun et al., 2016a), and plants are grown in climatically extreme environments and nutrient-poor conditions (Sun and Wang, 2016a). It makes the alpine grassland ecosystem on the Tibetan Plateau highly sensitive to climate change (Wang et al., 2007). In addition, the SR level

that was measured in the Tibetan Plateau is higher than in other regions at similar latitudes (Liu et al., 2012), which led to a more pronounced response of the plant due to the stronger photosynthesis rate induced by high SR (Liu et al., 2000). Furthermore, the high SR limited some of the soil properties, which, in turn, affect the nutrients provided by leaf N and P stoichiometry (Fan et al., 2011). Consequently, it is very informative to explore the mechanism of the effect of SR on leaf N and P stoichiometry across the alpine meadows of the Tibetan Plateau.

2. Materials and methods

2.1. Study area

Located in southwestern China, the Tibetan Plateau (26°00'–39°47'N, 73°19'–104°47'E), which is viewed as the “Third Pole”, is the highest and most extensive plateau in the world, with an average altitude exceeding 4000 m (Sun et al., 2013a) (Fig. 2). The overall climatic characteristics of the region are strong radiation, intense sunshine, low temperature and accumulated temperature (Sun and Qin, 2016; Sun et al., 2016b). Temperature and precipitation have distinct regional distribution patterns in this area, with a mean annual air temperature (MAT) ranging from -15 to 20 °C and a mean annual precipitation (MAP) ranging from 50 to 700 mm from the northwest to the southeast (Ma and Sun, 2018). The Tibetan Plateau is dominated by alpine meadow soil and subalpine meadow soil with abundant and fertile soil nutrients. Grasslands or land types of the Tibetan Plateau are dominated by alpine meadow, alpine steppe, alpine shrub grassland, and desert grassland (Sun et al., 2016a).

2.2. Sampling design and database creation

Sample collection and measurements were carried out in late July and early August of 2003, and nearly all of the measured plants were taken at the flowering stage. We selected 62 relatively evenly spaced sites along the transect by visual inspection of the alpine meadow area, and we tried to maintain the sample sites by allowing only minimal grazing while preventing other anthropogenic disturbances (Table 1). At each site, the dominant species were selected for measurement (He et al., 2006). We collected sun-exposed and newly mature leaves of five

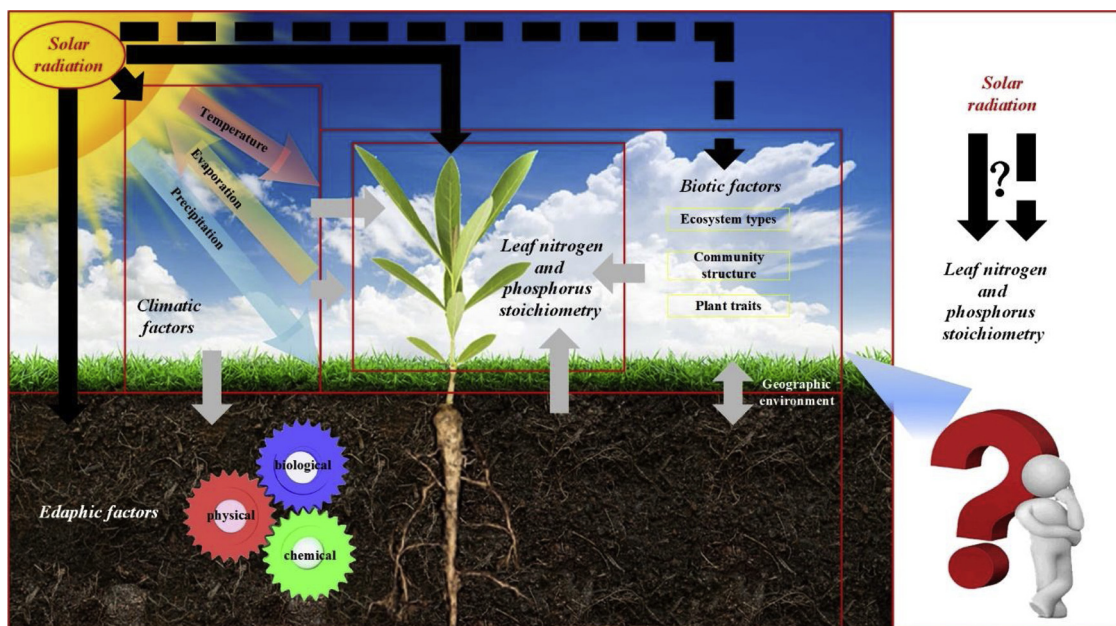


Fig. 1. The hypothetical model of the effect of solar radiation in determining dynamic patterns of leaf nitrogen and phosphorus stoichiometry in alpine meadow. According to the graph, dashed line and solid line represent indirectly and directly path. The single arrow represents a one-way effect while the double arrow represents an interaction.

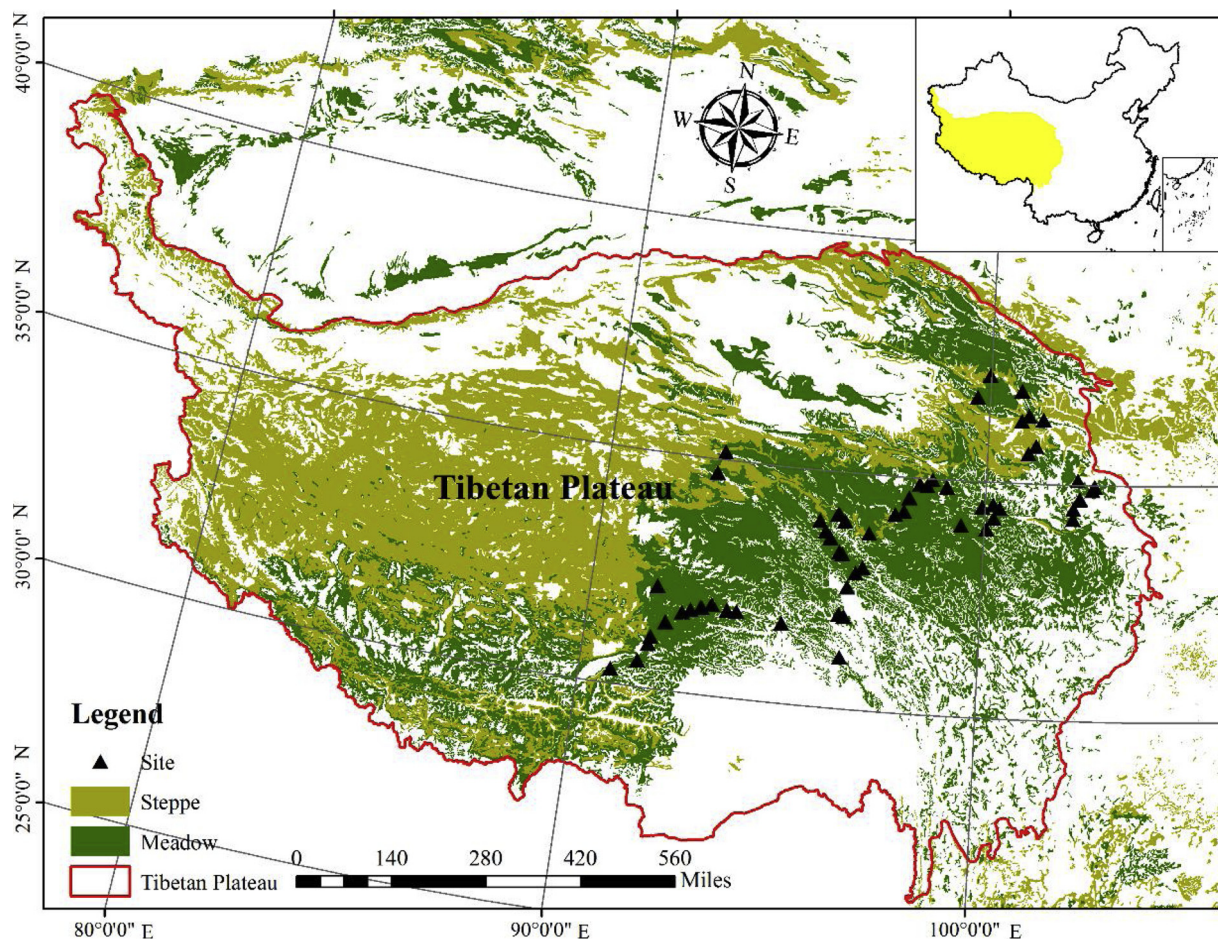


Fig. 2. Spatial distribution of sampling sites on the Tibetan Plateau, China. The black solid triangle represents the samples collected in alpine meadow. In addition, the yellow areas represent meadow while the green areas represent steppe (For interpretation of the references to colour in this figure legend, the reader is referred to the web version of this article).

to ten plants of each species at each site, placed them in paper envelopes, and dried them naturally. Samples were oven-dried at 60 °C upon returning to the laboratory. Then, the dried samples were ground by a ball mill (NM200, Retsch, Haan, Germany) until becoming fine powders.

We used an elemental analyser (2400 II CHNS/O Elemental Analyzer, Perkin-Elmer, USA) to measure the total leaf nitrogen concentration. Each sample was determined on 5–6 mg homogeneously ground material by providing an environment with a 950 °C combustion temperature and a 640 °C reduction temperature. In addition, we used H₂SO₄–H₂O₂–HF digestion quantified as a known phosphorus concentration (Bowman, 1988) in reference to a national standard material (reference code GBW08513; General Administration of Quality Supervision, People’s Republic of China). Then, we measured the total leaf P concentration by using a molybdate/stannous chloride method (He et al., 2008).

The climate dataset used in this study covers 30-year records (1970–2000), including the average temperature, precipitation and solar radiation, which were obtained from WorldClim Version2 (<http://worldclim.org>), and the soil dataset was obtained from ISRIC-World Soil Information, which is the host of the World Data Center for Soil (WDC-Soils) (Batjes, 2016). Then, we extracted values using ArcMap10.2 software (ESRI, Inc., Redlands, CA, USA).

2.3. Data analysis

The data of the leaf N and P concentrations we obtained were tested by Pauta Criterion to avoid data bias caused by external and man-made

factors in the process of data measurement. In addition, the testing formulas were as follows:

$$\begin{cases} \sigma = \sqrt{\frac{1}{n-1} \left[\sum_{i=1}^n \delta_i^2 - \frac{1}{n} \left(\sum_{i=1}^n \delta_i \right)^2 \right]} \\ \bar{L} = x_0 + \frac{1}{n} \left(\sum_{i=1}^n \delta_i \right) \\ \mu_i = |x_i - \bar{L}| > 3\sigma \end{cases} \quad (1)$$

In these formulas, $\delta_i = x_i - x_0$, where x_i represented the leaf N and P concentrations, and x_0 represented average leaf N and P concentrations. If the data error was greater than 3σ , they were removed. In addition, the data on the leaf N and P concentrations exhibited significant normal distribution, which was tested by the K–S method using SPSS22 software (SPSS, Inc., Chicago, IL, USA).

The boosted regression tree (BRT) is a self-directed learning method that is based on the classification regression tree. This method produces multiple regression trees by random selection and self-directed learning, which can improve the stability and prediction accuracy of the model (Cheong et al., 2014; Elith et al., 2008; Müller et al., 2013; R Core Team, 2015). In the process of operation, a certain amount of random data is extracted several times to analyse the influence of independent variables on dependent variables, and the remaining data are used to test the fitting results. Finally, the average of the resulting multiple regression was output as the result. The BRT can obtain the contribution rate of an independent variable to the dependent variable, and the relationship between a particular independent variable and a dependent variable when other independent variables remain unchanged or take the mean value (Buston and Elith, 2011). In this study,

Table 1

The information of sampled sites, Data for latitude, longitude and altitude were obtained by Magellan GPS Field PRO V (Magellan System Corporation, San Dimas, CA, USA). And mean annual temperature (MAT), mean annual precipitation (MAP) and solar radiation (SR) were calculated from 30-year records (1970–2000) at WorldClim Version2 (<http://worldclim.org>).

site	Longitude(°E)	Latitude(°N)	Altitude(m)	MAT(°C)	MAP(mm)	SR(kJ m ⁻² d ⁻¹)	dominant species
1	102.44	35.10	3097	2.38	566	14481.00	<i>Elymus nutans</i> , <i>Stipa aliena</i>
2	102.89	34.97	3019	2.73	571	14293.17	<i>Stipa aliena</i> , <i>Medicago lupulina</i> , <i>Thermopsis lanceolata</i> , <i>Saussurea</i> sp.
3	102.83	34.90	3256	1.64	592	14227.25	<i>Potentilla fruticosa</i> , <i>Hippophae thibetana</i> , <i>Polygonum viviparum</i>
4	102.34	34.49	3584	0.38	650	14041.75	<i>Polygonum viviparum</i> , <i>Kobresia parva</i> , <i>Kobresia capillifolia</i>
5	102.34	34.28	3494	1.00	647	14046.42	<i>Gentiana straminea</i> , <i>Kobresia parva</i>
6	102.49	34.70	3304	1.51	615	14166.58	<i>Potentilla fruticosa</i> , <i>Polygonum viviparum</i> , <i>Gentiana straminea</i> , <i>Salix ortrepha</i>
7	102.51	34.71	3292	1.56	614	14181.17	<i>Potentilla fruticosa</i> , <i>Elymus nutans</i> , <i>Ligularia sagitta</i>
8	100.89	36.32	3286	0.84	437	15547.75	<i>Achnatherum splendens</i>
9	100.40	34.45	4376	-4.12	587	14560.58	<i>Achnatherum splendens</i> , <i>Ceratoides latens</i> , <i>Achnatherum inebrians</i>
10	100.22	34.53	3774	-0.74	512	14992.50	<i>Ligularia virgaurea</i> , <i>Kobresia parva</i> , <i>Gentiana straminea</i> , <i>Polygonum viviparum</i>
11	99.93	34.47	3896	-1.73	497	15017.33	<i>Saussurea superba</i> , <i>Spiraea alpina</i> , <i>Gentiana straminea</i> , <i>Polygonum viviparum</i>
12	98.97	34.84	4510	-7.65	432	15127.92	<i>Kobresia tibetica</i> , <i>Saussurea graminifolia</i> , <i>Kobresia</i> sp., <i>Carex moorcroftii</i>
13	98.58	34.99	4299	-5.07	354	15608.08	<i>Saussurea graminifolia</i> , <i>Festuca rubra</i>
14	98.45	34.85	4227	-4.33	349	15656.17	<i>Elymus nutans</i> , <i>Cremanthodium discoideum</i> , <i>Microula tibetica</i>
15	98.25	34.88	4234	-3.45	331	15766.50	<i>Stipa purpurea</i> , <i>Kobresia kansuensis</i>
16	97.99	34.58	4282	-4.06	370	15666.08	<i>Kobresia tibetica</i> , <i>Carex moorcroftii</i>
17	97.02	33.76	4566	-5.69	527	15514.92	<i>Kobresia parva</i> , <i>Meconopsis integrifolia</i> , <i>Kobresia capillifolia</i>
18	96.37	33.97	4247	-2.49	454	15885.00	<i>Gentiana straminea</i> , <i>Oxytropis ochrocephala</i> , <i>Kobresia humilis</i>
19	96.20	34.10	4446	-4.10	454	15905.92	<i>Kobresia parva</i> , <i>Koeleria cristata</i> , <i>Oxytropis ochrocephala</i> , <i>Kobresia humilis</i>
20	95.70	33.95	4175	-1.65	430	16046.00	<i>Kobresia parva</i> , <i>Stellera chamaejasme</i>
21	95.88	33.73	4372	-2.57	485	15924.58	<i>Kobresia humilis</i> , <i>Stellera chamaejasme</i>
22	96.01	33.60	4440	-2.98	499	15886.83	<i>Potentilla parvifolia</i> , <i>Lamiophlomis rotata</i> , <i>Caragana jubata</i>
23	96.36	33.28	4287	-2.18	522	15748.92	<i>Kobresia parva</i>
24	96.91	33.02	4024	-0.27	518	15574.67	<i>Ligularia virgaurea</i> , <i>Kobresia parva</i> , <i>Artemisia sieversiana</i>
25	96.74	32.90	4346	-1.65	550	15504.58	<i>Gentiana straminea</i> , <i>Oxytropis ochrocephala</i> , <i>Potentilla parvifolia</i>
26	96.56	32.59	4040	1.75	532	15545.25	<i>Iris chinensis</i> , <i>Ligularia virgaurea</i> , <i>Stellera chamaejasme</i> , <i>Pedicularis alaschanica</i>
27	96.53	31.97	4153	0.45	559	15346.33	<i>Polygonum viviparum</i> , <i>Salix ortrepha</i> , <i>Potentilla parvifolia</i> , <i>Gnaphalium affine</i>
28	96.39	32.00	4213	-0.38	572	15334.92	<i>Rhododendron thymifolium</i> , <i>Spiraea alpina</i> , <i>Potentilla glabra</i> , <i>Salix</i> sp.
29	96.51	31.10	4716	-3.60	613	14937.58	<i>Rhododendron thymifolium</i> , <i>Cotoneaster adpressus</i> , <i>Rhododendron</i> sp
30	94.96	31.70	4384	-2.97	642	15404.33	<i>Rheum acetosa</i> , <i>Spiraea mongolica</i> , <i>Berberis diaphana</i> , <i>Primula tangutica</i>
31	93.79	31.84	4042	1.90	574	16304.92	<i>Berberis diaphana</i> , <i>Lonicera hispida</i> , <i>Gentiana straminea</i>
32	93.54	31.85	4495	-2.57	590	16183.83	<i>Kobresia parva</i> , <i>Potentilla parvifolia</i>
33	93.14	31.93	4479	-1.46	536	16393.42	<i>Kobresia parva</i>
34	92.90	31.84	4309	0.53	502	16570.58	<i>Kobresia</i> sp2, <i>Kobresia humilis</i>
35	92.87	31.83	4299	0.82	498	16605.17	<i>Kobresia parva</i> , <i>Kobresia humilis</i> , <i>Ptilagrostis dichotoma</i>
36	91.69	31.10	4750	-2.05	438	16735.25	<i>Kobresia tibetica</i>
37	90.81	30.31	4324	2.73	408	17,245.17	<i>Potentilla parvifolia</i>
38	101.48	36.37	3504	-2.02	532	15051.42	<i>Leontopodium pusillum</i> , <i>Gentiana leucomelaena</i> , <i>Potentilla fruticose</i>
39	101.30	35.80	3300	1.27	481	15187.67	<i>Anaphalis sinica</i> , <i>Artemisia frigida</i> , <i>Elymus nutans</i> , <i>Galium verum</i>
40	101.09	35.63	3740	-0.73	501	15070.08	<i>Kobresia humilis</i> , <i>Kobresia pygmaea</i> , <i>Melissitus</i>
41	100.25	34.24	4343	-4.05	578	14608.58	<i>Hedysarum macrophyllum</i> , <i>Polygonum macrophyllum</i> , <i>Polygonum viviparum</i>
42	100.07	34.01	4204	-3.84	580	14584.92	<i>Androsace mariae</i> , <i>Lagotis brachystachya</i> , <i>Ligularia</i>
43	99.40	34.06	4224	-3.76	506	14896.00	<i>Ligularia virgaurea</i>
44	98.00	34.57	4296	-4.17	373	15644.17	<i>Lancea tibetica</i> , <i>Meconopsis horridula</i> , <i>Stellaria media</i>
45	97.88	34.28	4650	-6.90	457	15310.50	<i>Agrostis matsumurae</i> , <i>Kobresia humilis</i> , <i>Kobresia tibetica</i>
46	96.28	33.32	4536	-4.28	542	15669.75	<i>Taraxacum mongolicum</i>
47	96.16	34.10	4444	-4.12	453	15909.75	<i>Saussurea sericea</i> , <i>Saussurea stoliczkae</i> , <i>Stipa aliena</i>
48	101.09	36.44	3492	-0.54	472	15382.92	<i>Gentiana szechenyii</i> , <i>Kobresia capillifolia</i> , <i>Kobresia humilis</i> , <i>Kobresia pygmaea</i>
49	100.86	36.95	3133	0.11	434	15807.75	<i>Artemisia dacunculoides</i> , <i>Bupleurum longicaule</i> , <i>Leymus secalinus</i> , <i>Stipa krylovii</i>
50	99.98	37.26	3217	0.38	346	16328.92	<i>Achnatherum splendens</i> , <i>Allium tanguticum</i> , <i>Potentilla saundersiana</i>
51	93.04	35.17	4680	-5.42	270	16344.75	<i>Festuca ovina</i> , <i>Kengyilia thoroldiana</i> , <i>Kobresia robusta</i> , <i>Leontopodium pusillum</i>
52	92.89	34.72	4811	-6.17	306	16253.17	<i>Androsace mariae</i> , <i>Kobresia humilis</i> , <i>Poa annua</i>
53	91.72	32.18	4877	-4.05	437	16656.83	<i>Carex moorcroftii</i> , <i>Littledealea racemosa</i> , <i>Potentilla pamiroalaica</i> , <i>Stipa purpurea</i>
54	91.72	32.18	4877	-4.05	437	16656.83	<i>Kobresia humilis</i> , <i>Kobresia pygmaea</i> , <i>Stipa regeliana</i>
55	92.02	31.45	4489	-0.31	426	16828.42	<i>Gentiana szechenyii</i> , <i>Lagotis brachystachya</i> , <i>Leontopodium leontopodioides</i>
56	92.02	31.44	4483	-0.27	426	16829.67	<i>Aster tataricus</i> , <i>Astragalus mattam</i> , <i>Gentiana szechenyii</i>
57	92.62	31.77	4658	-2.75	501	16442.17	<i>Kobresia pygmaea</i> , <i>Potentilla saundersiana</i> , <i>Slipa penicillata</i>
58	92.41	31.69	4603	-1.82	470	16564.42	<i>Primula fasciculata</i>
59	91.66	30.94	4764	-2.15	434	16830.00	<i>Poa indattenuata</i> , <i>Stipa purpurea</i>
60	91.45	30.56	4524	0.53	421	16966.42	<i>Kobresia pygmaea</i> , <i>Thalictrum alpinum</i>
61	90.80	30.31	4324	2.73	408	17,245.17	<i>Astragalus strictus</i> , <i>Kobresia vidua</i> , <i>Stipa capillacea</i>
62	99.67	36.78	3395	-0.78	319	16196.33	<i>Elymus nutans</i> , <i>Melissitus ruthemica</i> , <i>Polygonum</i>
range	90.80°102.89	30.31°37.26	3019°4877	-7.65°2.73	270°650	14041.75°17,245.17	

a BRT analysis was conducted on the leaf N and P concentrations to ascertain the relative influences of environmental factors, including the SR, MAP, MAT, soil P concentrations (SP), soil organic carbon (SOC), available water capacity (TAWC), cation exchange capacity (CEC) and total soil nitrogen (STN).

Relationships between the leaf N and P stoichiometry and

environmental factors in alpine meadows were visualized in scatter plots based on SigmaPlot10.0 software (2006 Systat Software, Inc., Chicago, IL, USA). To explore the relationships between climatic factors and soil factors, we carried out the correlation matrix diagram and exhibited it in R software 3.4.1 (R Core Team, 2015).

Structural equation modelling (SEM) is a multivariate technique

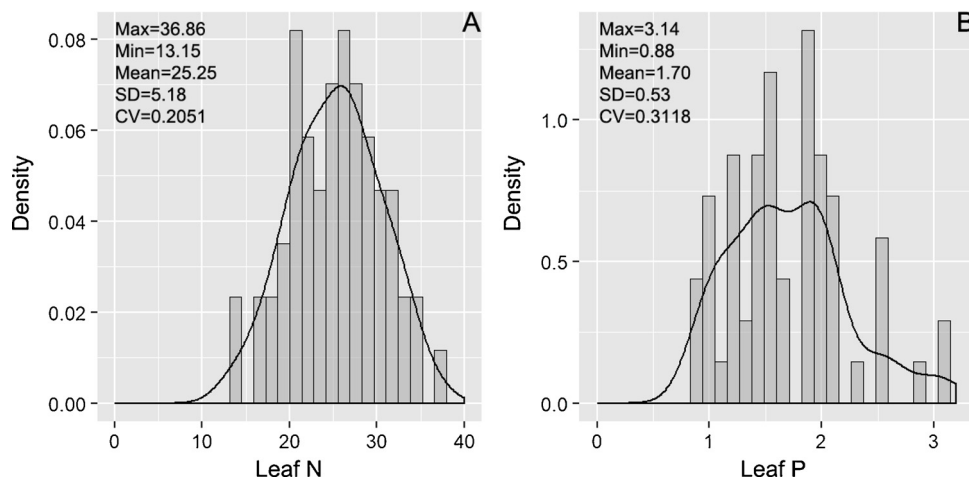


Fig. 3. Density distributions of leaf nitrogen (A) and leaf phosphorus (B) stoichiometry in alpine meadow.

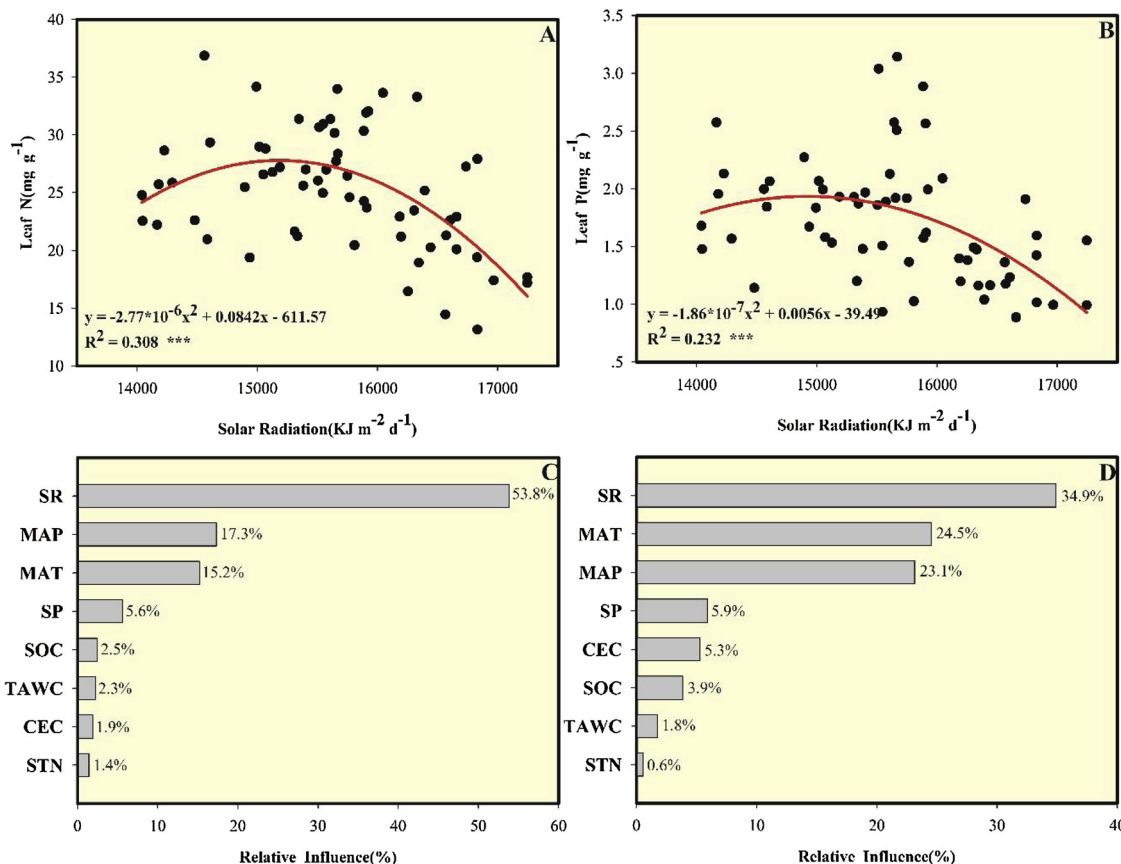


Fig. 4. Relationships of solar radiation with leaf nitrogen (A) and leaf phosphorus (B), and the relative influence of each driving factor on leaf nitrogen (C) and leaf phosphorus (D). *** represent correlation is significant at the 0.001 level.

that involves computer algorithms and statistical methods (Gupta et al., 2017; Li et al., 2018). We used it to test the direct and indirect effects on leaf N and P stoichiometry and to describe the hypothetical causal relationships (Fan et al., 2016). By selecting the appropriate variables and models based on certain statistical criteria (Sun et al., 2018), the standard estimating results expressed the influence on the different factors by the path coefficients, and validation of the model was conducted in the AMOS statistical tool (17.0.2, Amos Development Corporation, Crawfordville, FL, USA).

3. Results

3.1. Leaf N and leaf P across alpine meadow

The leaf N and leaf P ranged from 13.15 to 36.86 mg g⁻¹ to 0.88–3.14 mg g⁻¹, which exhibited large variations in our results (Fig. 3). The corresponding mean values were 25.25 mg g⁻¹ and 1.70 mg g⁻¹ across all sites; the standard errors (SD) were 5.18 mg g⁻¹ and 0.53 mg g⁻¹, respectively; and the coefficients of variations (CV) were 0.21 and 0.31, respectively. All results followed normal distribution.

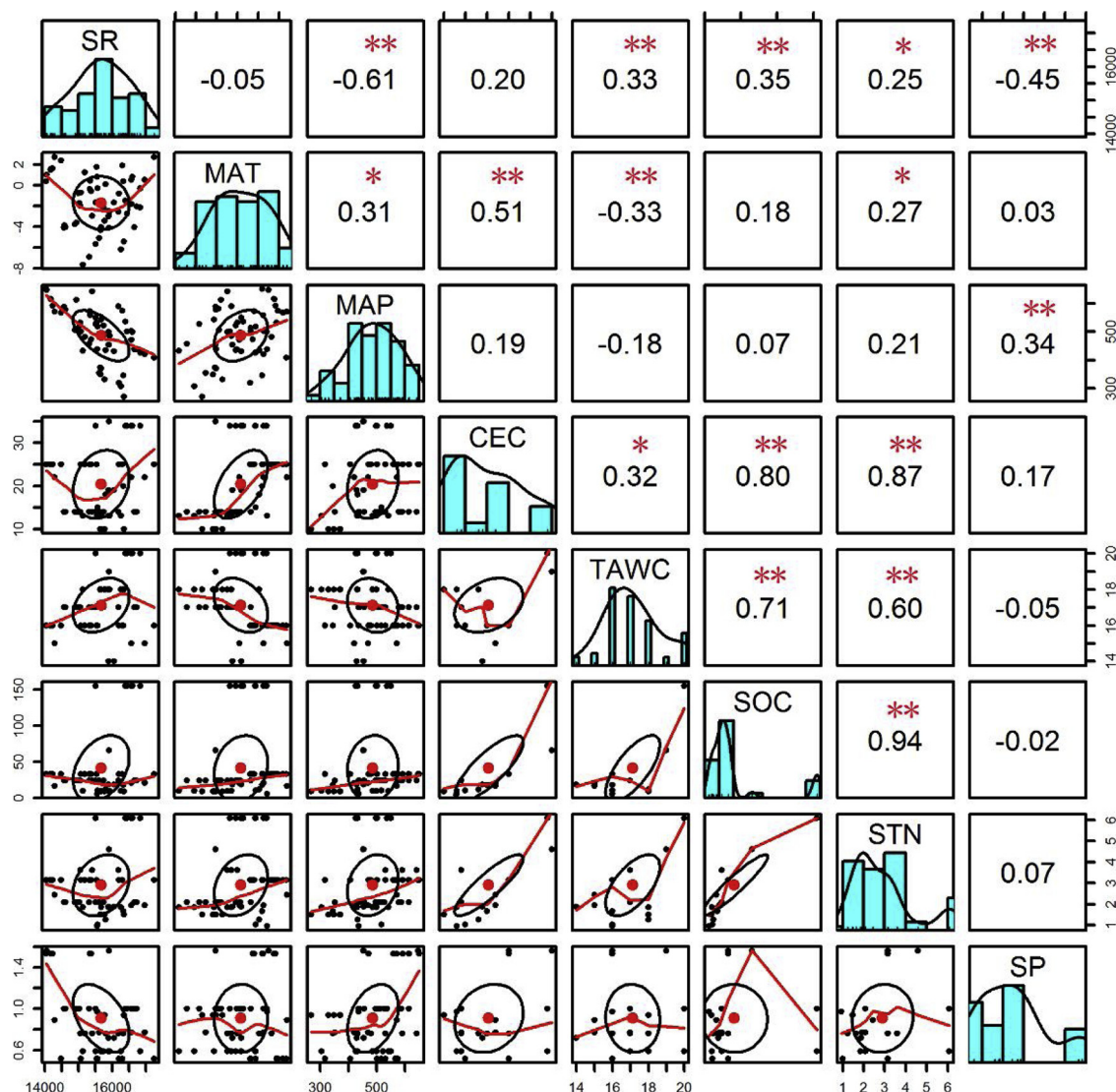


Fig. 5. Correlation of all climate and soil factors at alpine meadow. Climate factors including solar radiation (SR), mean annual temperature (MAT) and mean annual precipitation (MAP); and soil factors including cation exchange capacity (CEC), available water capacity (TAWC), soil organic carbon (SOC), total soil nitrogen (STN) and soil P concentrations (SP); scatter plots in the lower left represented the relationships about different factors, and red line represented fit relationships; histogram plots in the center section represented normal distribution; and data in the upper right represented correlation and significance level. * represent $p < 0.05$, ** represent $p < 0.01$ (For interpretation of the references to colour in this figure legend, the reader is referred to the web version of this article).

3.2. Analysis of the driving factors of leaf N and leaf P

The influence of climatic factors, biotic factors and edaphic factors on the leaf nitrogen and phosphorus stoichiometry was analysed by a boosted regression tree (BRT). Fig. 4C and D illustrate the influence of these factors on the leaf N and leaf P. For both leaf N (Fig. 4C) and leaf P (Fig. 4D), SR ranks as the greatest relative influence among all 8 driving factors. Their contribution rates reached 53.8% and 34.9%, respectively. For the leaf N, other driving factors are MAP, MAT, SP, SOC, TAWC, CEC and STN, which is in order from greatest to least, and their relative influences are 17.3%, 15.2%, 5.6%, 2.5%, 2.3%, 1.9% and 1.4%, respectively. For the leaf P, the other driving factors followed by MAT, MAP, SP, CEC, SOC, TAWC and STN with relative influence are 24.5%, 23.2%, 5.9%, 5.3%, 3.9%, 1.8% and 0.6%, respectively.

In addition, the regression analysis showed a quadratic curve relation between the SR and leaf nitrogen and phosphorus stoichiometry (Leaf N: $y = -2.77 \times 10^{-6}x^2 + 0.0842x - 611.57$, $R^2 = 0.31$, $p < 0.001$; Leaf P: $y = -1.86 \times 10^{-7}x^2 + 0.0056x - 39.49$, $R^2 = 0.23$, $p < 0.001$) (Fig. 4). Coincidentally, the optimal values of solar radiation (leaf N: $15,198 \text{ KJ m}^{-2} \text{ d}^{-1}$; leaf P: $15,053 \text{ KJ m}^{-2} \text{ d}^{-1}$) for leaf N and

P are almost equal, which means that when the values of solar radiation are greater than $15,000 \text{ KJ m}^{-2} \text{ d}^{-1}$, the leaf N and P are negative with SR.

3.3. Linkages between climatic factors and soil factors

The SR was significantly correlated to several environmental factors (Fig. 5), including MAP ($R^2 = 0.61$, $p < 0.01$), TAWC ($R^2 = 0.33$, $p < 0.01$), SOC ($R^2 = 0.35$, $p < 0.01$), STN ($R^2 = 0.25$, $p < 0.05$), and SP ($R^2 = 0.45$, $p < 0.01$); however, SR was non-significantly correlated to MAT and CEC. Meanwhile, MAT was significantly correlated to MAP ($R^2 = 0.31$, $p < 0.05$), CEC ($R^2 = 0.51$, $p < 0.01$), TAWC ($R^2 = 0.33$, $p < 0.01$), and STN ($R^2 = 0.27$, $p < 0.05$), whereas CEC was also significantly correlated to TAWC ($R^2 = 0.32$, $p < 0.05$), SOC ($R^2 = 0.80$, $p < 0.01$) and STN ($R^2 = 0.87$, $p < 0.01$). Obviously, complex interactions among various environmental factors were shown in the correlation matrix diagram across the alpine meadows of the Tibetan Plateau.

Table 2

Summary of the direct, indirect and total effects of variables (Solar Radiation, MAP, MAT, TAWC, CEC, SOC, STN, SP, Leaf N and Leaf P) in the SEM of alpine meadow. Effects were calculated with standardized path coefficients.

Standardized Direct Effects										
Variable	Solar Radiation	MAP	MAT	TAWC	CEC	SOC	STN	SP	Leaf N	Leaf P
MAP	-.615	.000	.000	.000	.000	.000	.000	.000	.000	.000
MAT	.235	.459	.000	.000	.000	.000	.000	.000	.000	.000
TAWC	.441	.213	-.375	.000	.000	.000	.000	.000	.000	.000
CEC	.187	.192	.623	.493	.000	.000	.000	.000	.000	.000
SOC	.159	.143	.014	.504	.573	.000	.000	.000	.000	.000
STN	.055	.168	-.042	.115	.405	.508	.000	.000	.000	.000
SP	-.427	.087	-.252	.169	.757	-.551	.000	.000	.000	.000
Leaf N	-.293	-.118	.000	.000	.000	.274	-.328	.000	.000	.402
Leaf P	-.343	.000	-.281	.000	.000	-.065	.000	-.024	.148	.000
Standardized Indirect Effects										
Variable	Solar Radiation	MAP	MAT	TAWC	CEC	SOC	STN	SP	Leaf N	Leaf P
MAP	.000	.000	.000	.000	.000	.000	.000	.000	.000	.000
MAT	-.282	.000	.000	.000	.000	.000	.000	.000	.000	.000
TAWC	-.114	-.172	.000	.000	.000	.000	.000	.000	.000	.000
CEC	.014	.306	-.185	.000	.000	.000	.000	.000	.000	.000
SOC	.191	.313	.062	.283	.000	.000	.000	.000	.000	.000
STN	.196	.419	.173	.599	.291	.000	.000	.000	.000	.000
SP	-.028	.018	.226	-.060	-.316	.000	.000	.000	.000	.000
Leaf N	-.072	-.148	-.145	-.042	-.096	-.182	-.021	-.010	.063	.025
Leaf P	-.053	-.201	-.026	-.060	-.062	.027	-.052	-.002	.009	.063
Standardized Total Effects										
Variable	Solar Radiation	MAP	MAT	TAWC	CEC	SOC	STN	SP	Leaf N	Leaf P
MAP	-.615	.000	.000	.000	.000	.000	.000	.000	.000	.000
MAT	-.047	.459	.000	.000	.000	.000	.000	.000	.000	.000
TAWC	.327	.041	-.375	.000	.000	.000	.000	.000	.000	.000
CEC	.201	.498	.438	.493	.000	.000	.000	.000	.000	.000
SOC	.351	.456	.076	.786	.573	.000	.000	.000	.000	.000
STN	.250	.587	.131	.714	.696	.508	.000	.000	.000	.000
SP	-.455	.105	-.025	.109	.442	-.551	.000	.000	.000	.000
Leaf N	-.365	-.266	-.145	-.042	-.096	.092	-.348	-.010	.063	.427
Leaf P	-.396	-.201	-.307	-.060	-.062	-.039	-.052	-.025	.158	.063

Note: MAP, MAT, TAWC, CEC, SOC, STN and SP represent mean annual precipitation, mean annual temperature, available water capacity, cation exchange capacity, soil organic carbon, soil total nitrogen and soil P concentrations, respectively.

3.4. The direct and indirect effects of environmental factors on the leaf nitrogen and phosphorus contents

The final SEM explained 40.4% of the variation in the leaf N and 36.6% of the variation in the leaf P in the alpine meadow. Table 2 shows a summary of the direct, indirect, and total effects of the variables. Increasing solar radiation, MAT, SP and SOC are strongly associated with decreases in the leaf P, which indicates that leaf P could be well-predicted from these four variables ($R^2 = 0.366$). Even though there were significant bivariate relationships among MAP, CEC, TAWC, STN and leaf P, the results mostly indicated the indirect negative effects on leaf P. The rank of total effects, in decreasing order, was solar radiation, MAT, MAP, CEC, TAWC, STN, SOC and SP (Table 2). Meanwhile, leaf N has received negative effects from solar radiation, MAP and SP, but it is positive with SOC, which indicates that leaf N could be well-predicted from these four variables ($R^2 = 0.404$). In addition, MAT, CEC, TAWC, and SP had only an indirect negative effect on leaf N through its direct effect or its indirect effect on MAP, STN and SOC. The rank of the total effects, in decreasing order, was solar radiation, STN, MAP, MAT, CEC, SOC, TAWC and SP (Table 2).

It is also evident that leaf N and leaf P can be predicted from solar radiation and other environmental factors, with solar radiation explaining the largest percentage of the variation.

4. Discussion

4.1. The mechanism by which solar radiation regulates leaf nitrogen and phosphorus stoichiometry

The debate over leaf nitrogen and phosphorus stoichiometry is ongoing, and previous studies generally hold that the variations of leaf N and P concentrations are controlled by several environmental factors such as MAT and MAP (Güsewell, 2004). MAT and MAP are two important factors that affect plant growth across the alpine meadow in the Tibetan Plateau, which has already been shown (Li et al., 2011; Zhuo, 2017), and both MAT and MAP had significant correlations with leaf N and P concentrations (Ordoñez et al., 2009; Reich and Oleksyn, 2004; Sinclair et al., 2000). Unlike the previous studies, this study reveals a strong correlation among SR, leaf nitrogen and phosphorus stoichiometry, and it verifies the hypothesis that solar radiation regulates leaf nitrogen and phosphorus stoichiometry across alpine meadows.

Although the relative influences of MAP and MAT to leaf nitrogen and phosphorus stoichiometry were all higher than 15% in our experiments, SR had the greatest effects on both leaf N and P concentrations (Fig. 4). As a climatic factor, the direct effects of SR on plant growth and photosynthesis cannot be ignored (Xing et al., 2017). A large number of studies have shown that SR is the most direct and important climatic factor affecting plant growth and development (Christian and Jeanclaude, 2008). The spectrum, duration of sunshine and illumination intensity are direct tools of SR at work. For the

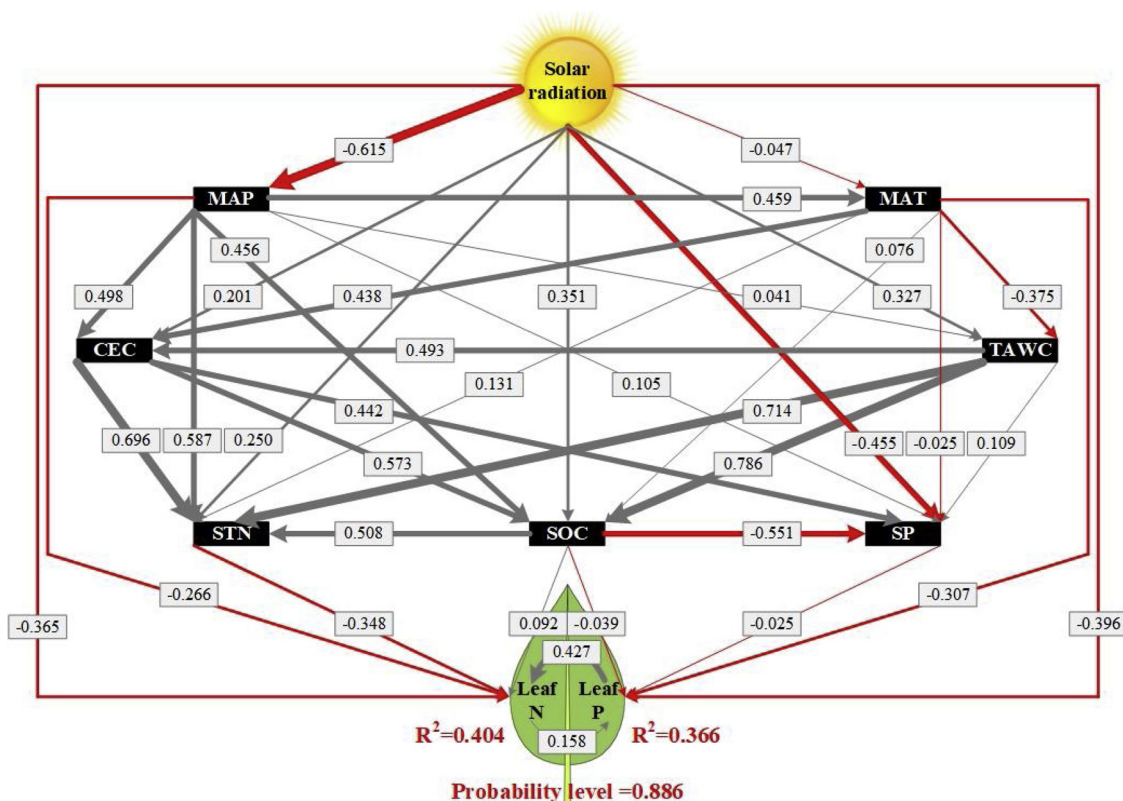


Fig. 6. Using the SEM to analyze the directly and indirectly effects among variables in alpine meadow. The standardized total coefficients are listed on each significant path. The thickness of the solid arrows reflects the magnitude of the standardized SEM coefficients, the gray solid line represents the positive effect while the red solid line represents the negative effect. MAP, MAT, TAWC, CEC, SOC, STN and SP represent mean annual precipitation, mean annual temperature, available water capacity, cation exchange capacity, soil organic carbon, soil total nitrogen and soil P concentrations, respectively (For interpretation of the references to colour in this figure legend, the reader is referred to the web version of this article).

spectrum, UVA rays can stimulate the growth of plants, boost plant productivity and promote the synthesis of protein, sugar and acid (Caldwell, 1981; Mazza et al., 2000). While UVC rays suppress the growth of the plant, which prevents plants from growing unusually fast, they also possess the function of disinfection and sterilization, which can reduce plant diseases (Herrmann et al., 2010). At the same time, visible light is the raw material by which green plants accumulate organic matter during photosynthesis, and the thermal effect produced by far-infrared rays can supply heat for plant growth and development (Wiegand and Namken, 1966). However, for duration of sunshine, visible light mainly affects the flowering, fruiting and dormant stages of plants through the alternation of daytime light and night-time darkness (Christian and Jeanclaude, 2008), and all physiological processes of plants affect the accumulation of leaf N and P. In addition, the illumination intensity has the greatest influence on plant growth and development. It directly affects the intensity of plant photosynthesis. Chang et al. (2008) suggested that decreased illumination intensity usually reduces the stomatal conductance and then reduces the net photosynthetic rate, thus resulting in a decline in the yield and quality of plants (Zheng et al., 2012a). In a certain range of illumination intensity, the intensity of photosynthesis increases with the increasing illumination intensity (Duriyaprapan and Britten, 1982). Several studies have also demonstrated that the appropriate illumination intensity level promotes the accumulation of dry matter and contributes to a high yield (Katsura et al., 2008). However, when the illumination intensity exceeds the saturation point of light, it will lower the activity of photosynthesis enzymes and damage the plant growth hormones, thus leading to photoinhibition (Xu et al., 1992). In addition, intense illumination intensity can also destroy the protoplasm, causing chlorophyll decomposition or the cells to lose too much water and close the stomata, thus resulting in the weakening or even ceasing of photosynthesis

(Getter et al., 2009; Maaikay et al., 2007; Szeicz, 1974). These processes are consistent with the quadratic curve relationship between SR and leaf nitrogen and phosphorus stoichiometry ($R^2 = 0.30, p < 0.001$, $R^2 = 0.23, p < 0.001$, respectively) across the Tibetan Plateau (Fig. 4). Because the leaf N concentration is controlled by the influence of the specific leaf area on photosynthesis (Reich et al., 1998) and the relative growth rate (Vanni et al., 2002), the leaf dry matter content also has a significant correlation with the leaf P concentration (Wu et al., 2012). In addition, high levels of nitrogen and phosphorus concentrations are also positive indicators of the high production rates of organelles and molecules (Delgado-Baquerizo et al., 2016). However, a high SR level was measured in the study area (Liu et al., 2012), and together with the simultaneously existing complex environment, the light saturation point can easily be reached, which causes photoinhibition in the photosynthesis process (Xu et al., 1992). In short, the SR levels at most of the sites in the study area are over $15,000 \text{ KJ m}^{-2} \text{ d}^{-1}$ (Table 1); on the whole, the leaf N and P are negative with SR (Fig. 6).

According to the structural equation model (Fig. 6 and Table 2), the regulation of SR on the leaf N and P stoichiometry is not merely reflected in the direct effects (path coefficient = -0.293 and -0.343, respectively) of the physiological process. The indirect effect (path coefficient = -0.072 and -0.053, respectively) was also revealed in the influence of SR on other environmental factors, such as precipitation, temperature, soil organic carbon, soil nitrogen and phosphorus. Consistent with many previous verified results (Fan et al., 2018; Vargo et al., 2018), this study shows a significant negative correlation between SR and MAP ($R^2 = 0.61, p < 0.01$). In the Tibetan Plateau, a high SR level and altitude are the main reasons for a lower MAT and MAP in areas of the Tibetan Plateau (Ouyang et al., 1998) (Table 1). The decreased soil eluviation reduced the losses of nutrients from leaf and soil, which resulted in an increase of the soil organic carbon and

soil N content (Esmeijer-Liu et al., 2009; Ni et al., 2001), for which the reaction mechanism is completely consistent with our SEM results (Fig. 6 and Table 2). Except for MAT and MAP, SR is also closely related to edaphic factors. In our study, we found that SR was significantly positive correlated to SOC ($R^2 = 0.35$, $p < 0.01$), STN ($R^2 = 0.25$, $p < 0.05$), as it slowed down the decomposition rate of SOC and STN (Li et al., 2018a; Qi et al., 2016) via forbidding the activities of the soil enzyme. There is no doubt that these edaphic factors often had effects on the leaf N and P stoichiometry. For example, some reports hold that the leaf N concentration had a significantly positive relationship with STN (Sun et al., 2017; Wang et al., 2015), and the leaf P concentration had a significantly positive relationship with SP (Debnath et al., 2011). However, in our study, STN had a negative effect on the leaf N concentration (Table 2), which indicated that STN was not a limiting factor for the leaf N concentration across the alpine meadow of the Tibetan Plateau, and the leaf N concentration was more prone to a species trait (Luo et al., 2015). Interestingly, the relationship between the leaf P concentration and the SP in this study is also inconsistent with these reports. The result might be due to the low concentration of P in Chinese soil, which inhibits the accumulation of leaf P; it is well known that the growth of terrestrial plants in China is generally restricted by the soil P concentration (Han et al., 2005). To summarize, many linkages were found among climatic elements, edaphic factors, and the leaf N and P stoichiometry, but SR plays a critical role in the leaf N and P stoichiometry of the alpine meadows of the Tibetan Plateau.

4.2. Limitations of the current study

As we know, SR is a key factor that directly affects plant physiological processes; those processes include plant growth, photosynthesis and a flowering phase (Chang et al., 2008; Xing et al., 2017). For example, in the photosynthesis process, plant leaves produce adenosine triphosphate and some phosphatases, such as a reduced coenzyme, which is correlated with the leaf P (Dai et al., 2009). However, in our study, the lack of some related tests makes it difficult for those physiological processes to be exhibited. Furthermore, in the process of indirect effect of SR on the leaf N and P stoichiometry, many other factors play a role in addition to climatic and edaphic variables, such as SR being proven to be correlated with rough terrain, and rough terrain also being correlated with leaf N and P stoichiometry (Liu et al., 2018; Zeng et al., 2008). Hence, we can pay more attention to the plant physiological process experiment to verify the effect of SR on the leaf N and P stoichiometry, and we should consider more measurable variables in the future.

5. Conclusion

In this study, we verified that SR affected the leaf N and P stoichiometry across alpine meadows of the Tibetan Plateau. SR influenced plant physiological processes by influencing plant growth and photosynthesis, thus causing different plant traits, which then affected the leaf N and P concentrations directly. Furthermore, the changed SR had a close relationship with other climatic and edaphic factors, which also played an important role in the leaf N and P concentrations. It was concluded that the physiology of alpine botany should be explored in the future to explain the mechanism of leaf N and P stoichiometry in depth.

Acknowledgements

This work was supported by the State Key Research Development Program of China (Grant No. 2016YFC0501803) and Science and Technology Service Network Initiative (KFJ-STS-ZDTP-036). We are grateful to Prof. Jinsheng He for supporting Data.

References

- Batjes, N., 2016. Harmonised soil property values for broad-scale modelling (WISE30sec) with estimates of global soil carbon stocks. *Geoderma* 269, 61–68.
- Bowman, R.A., 1988. A rapid method to determine total phosphorus in soils. *Soil Sci. Soc. Am. J.* 52 (5), 1301–1304.
- Buston, P.M., Elith, J., 2011. Determinants of reproductive success in dominant pairs of clownfish: a boosted regression tree analysis. *J. Anim. Ecol.* 80 (3), 528–538.
- Caldwell, M.M., 1981. Plant Response to Solar Ultraviolet Radiation.
- Chang, X., Alderson, P.G., Wright, C.J., 2008. Solar irradiance level alters the growth of basil (*Ocimum basilicum* L.) and its content of volatile oils. *Environ. Exp. Bot.* 63 (1–3), 216–223.
- Chen, Y., Han, W., Tang, L., Tang, Z., Fang, J., 2013. Leaf nitrogen and phosphorus concentrations of woody plants differ in responses to climate, soil and plant growth form. *Ecography* 36 (2), 178–184.
- Cheong, Y.L., Leitão, P.J., Lakes, T., 2014. Assessment of land use factors associated with dengue cases in Malaysia using boosted regression trees. *Spatial Spatio-temp. Epidemiol.* 10, 75.
- Christian, P., Jeanclaude, G., 2008. Efficient assessment of topographic solar radiation to improve plant distribution models. *Agric. For. Meteorol.* 148 (11), 1696–1706.
- Dai, Y.J., et al., 2009. Effects of shade treatments on the photosynthetic capacity, chlorophyll fluorescence, and chlorophyll content of *Tetragymma hemsleyanum* Diels et Gilg. *Environ. Exp. Bot.* 65 (3), 177–182.
- Debnath, A., Barrow, N.J., Ghosh, D., Malakar, H., 2011. Diagnosing P status and P requirement of tea (*Camellia sinensis* L.) by leaf and soil analysis. *Plant Soil* 341 (1–2), 309–319.
- Delgado-Baquerizo, M., Reich, P.B., García-Palacios, P., Milla, R., 2016. Biogeographic bases for a shift in crop C:N:P stoichiometries during domestication. *Ecol Lett* 19 (5), 564–575.
- Duan, J., Guo, S., 1992. Effect of shading and covering on the ecological environment of tea garden. *J. Anhui Agric. Coll.* 19 (3), 189–195.
- Duriyaprapan, S., Britten, E.J., 1982. The effects of solar radiation on plant growth, oil yield and oil quality of Japanese mint. *J. Exp. Bot.* 33 (137), 1319–1324.
- Elith, J., Leathwick, J.R., Hastie, T., 2008. A working guide to boosted regression trees. *J. Anim. Ecol.* 77 (4), 802–813.
- Esmeijer-Liu, A.J.A., Aerts, R., Kcorschner, W.M., Bobbink, R., Lotter, A.F., Verhoeven, J.T.A., 2009. Nitrogen enrichment lowers *Betula pendula* green and yellow leaf stoichiometry irrespective of effects of elevated carbon dioxide. *Plant Soil* 316 (1–2), 311–322.
- Fan, Y., Zhang, X., Wang, J., Shi, P., 2011. Effect of solar radiation on net ecosystem CO₂ exchange of alpine meadow on the Tibetan Plateau. *J. Geogr. Sci.* 21 (4), 92–102.
- Fan, Y., et al., 2016. Applications of structural equation modeling (SEM) in ecological studies: an updated review. *Ecol. Process.* 5 (1), 19.
- Fan, J., et al., 2018. Evaluation and development of temperature-based empirical models for estimating daily global solar radiation in humid regions. *Energy* 144, 903–914.
- Getter, K.L., Rowe, D.B., Cregg, B.M., 2009. Solar radiation intensity influences extensive green roof plant communities. *Urban For. Urban Green.* 8 (4), 269–281.
- Goulden, M.L., et al., 1997. Physiological responses of a black spruce forest to weather. *J. Geophys. Res. Atmos.* 102 (D24), 28987–28996.
- Gupta, V., Kapur, P.K., Kumar, D., 2017. Modeling and measuring attributes influencing DevOps implementation in an enterprise using structural equation modeling. *Inf. Softw. Technol.* 92, 75–91.
- Güsewell, S., 2004. N:P ratios in terrestrial plants: variation and functional significance. *New Phytol.* 164 (2), 243–266.
- Han, W., Fang, J., Guo, D., Zhang, Y., 2005. Leaf nitrogen and phosphorus stoichiometry across 753 terrestrial plant species in China. *New Phytol.* 168 (2), 377–385.
- He, J.S., et al., 2006. Stoichiometry and large-scale patterns of leaf carbon and nitrogen in the grassland biomes of China. *Oecologia* 149 (1), 115–122.
- He, J.S., Wang, L., Flynn, D.F.B., Wang, X., 2008. Leaf nitrogen:phosphorus stoichiometry across Chinese grassland biomes. *Oecologia* 155, 301–310.
- Hedin, L.O., 2004. Global organization of terrestrial plant-nutrient interactions. *Proc. Natl. Acad. Sci. U. S. A.* 101 (30), 10849–10850.
- Herrmann, H., Häder, D.P., Ghetti, F., 2010. Inhibition of photosynthesis by solar radiation in *Dunaliella salina*: relative efficiencies of UV-B, UV-a and PAR. *Plant Cell Environ.* 20 (3), 359–365.
- Hobbie, S.E., Gough, L., 2002. Foliar and soil nutrients in tundra on glacial landscapes of contrasting ages in northern Alaska. *Oecologia* 131 (3), 453–462.
- Kang, H., et al., 2011. Variation in leaf nitrogen and phosphorus stoichiometry in *Picea abies* across Europe: an analysis based on local observations. *For. Ecol. Manag.* 261 (2), 195–202.
- Katsura, K., et al., 2008. The high yield of irrigated rice in Yunnan, China: 'a cross-location analysis'. *Field Crops Res.* 107 (1), 1–11.
- Law, B.E., et al., 2002. Environmental controls over carbon dioxide and water vapor exchange of terrestrial vegetation. *Agric. For. Meteorol.* 113 (1), 97–120.
- Li, Y., Mao, W., Zhao, X., Zhang, T., 2010. Leaf nitrogen and phosphorus stoichiometry in typical desert and desertified regions, North China. *Environ. Sci.* 31 (8), 1716–1725.
- Li, L., Wang, Z., Xu, W., Wang, Q., 2011. Response of growth of typical plateau meadow on Tibetan Plateau to climate change. *J. Glaciol. Geocryol.* 33 (5), 1006–1013.
- Li, X., Chen, W., Cundy, A.B., Chang, A.C., Jiao, W., 2018. Analysis of influencing factors on public perception in contaminated site management: simulation by structural equation modeling at four sites in China. *J. Environ. Manage.* 210, 299–306.
- Liu, Z., Yang, J., Liu, X., 2000. Effects of several environmental factors on plant physiology in Qinghai-Xizang Plateau. *J. Desert Res.* 20 (3), 309–313.
- Liu, J., et al., 2012. Observation and calculation of the solar radiation on the Tibetan Plateau. *Energy Convers. Manage.* 57 (2), 23–32.

- Liu, Y., Wang, Q., Xin, Y., 2018. Ecological stoichiometry characteristics of temperate forest leaves: a review. *Chin. Agric. Sci. Bull.* 34 (10), 95–100.
- Luo, M., et al., 2015. C, N, P stoichiometry of plant and soil in the restorable plant communities distributed on the Land used for Qinghai-Tibet highway construction in the Qinghai-Tibetan Plateau. *Acta Ecol. Sin.* 35 (23), 7832–7841.
- Ma, B., Sun, J., 2018. Predicting the distribution of *Stipa purpurea* across the Tibetan Plateau via the MaxEnt model. *BMC Ecol.* 18 (1), 10.
- Maaikay, B., Isabel, V.G., Max, R., 2007. High solar radiation hinders tree regeneration above the alpine treeline in northern Ecuador. *Plant Ecol.* 191 (1), 33–45.
- Manzoni, S., Trofymow, J.A., Jackson, R.B., Porporato, A., 2010. Stoichiometric controls on carbon, nitrogen, and phosphorus dynamics in decomposing litter. *Ecol. Monogr.* 80 (1), 89–106.
- Mazza, C.A., Boccalandro, H.E., Giordano, C.V., Battista, D., Scopel, A.L., 2000. Functional significance and induction by solar radiation of ultraviolet-absorbing sunscreens in field-grown soybean crops. *Plant Physiol.* 122 (4) 1461–1461.
- Müller, D., Leitão, P.J., Sikor, T., 2013. Comparing the determinants of cropland abandonment in Albania and Romania using boosted regression trees. *Agric. Syst.* 117 (7), 66–77.
- Ni, J., Zhang, X.S., Scurlock, J.M.O., 2001. Synthesis and analysis of biomass and net primary productivity in Chinese forests. *Ann. For. Sci.* 58 (4), 351–384.
- Noymeir, I., 1973. Desert ecosystems: environment and producers. *Annu. Rev. Ecol. Syst.* 4 (1), 25–51.
- Ordoñez, J.C., et al., 2009. A global study of relationships between leaf traits, climate and soil measures of nutrient fertility. *Global Ecol. Biogeogr.* 18 (2), 137–149.
- Ouyang, J., Chen, Y., Du, J., Lu, F., 1998. On the correlation between the solar irradiance values and the precipitation values in China. *Sci. Meteorol. Sin.* 18 (1), 35–41.
- R Core Team, 2015. R: a Language and Environment for Statistical Computing 1. pp. 12–21.
- Reich, P.B., Oleksyn, J., 2004. Global patterns of plant leaf N and P in relation to temperature and latitude. *Proc. Natl. Acad. Sci. U. S. A.* 101 (30), 11001.
- Reich, P.B., Ellsworth, D.S., Walters, M.B., 1998. Leaf structure (specific leaf area) modulates photosynthesis-nitrogen relations: evidence from within and across species and functional groups. *Funct. Ecol.* 12 (6), 948–958.
- Ren, W., et al., 2003. Effect of low-light stress on nitrogen accumulation, distribution and grains protein content of *Indica* hybrid. *Plant Nutr. Fertil. Sci.* 9 (3), 288–293.
- Sinclair, T.R., et al., 2000. Leaf nitrogen concentration of wheat subjected to elevated [CO₂] and either water or N deficits. *Agric. Ecosyst. Environ.* 79 (1), 53–60.
- Sun, J., Qin, X.J., 2016. Precipitation and temperature regulate the seasonal changes of NDVI across the Tibetan Plateau. *Environ. Earth Sci.* 75 (4).
- Sun, J., Wang, H., 2016a. Soil nitrogen and carbon determine the trade-off of the above- and below-ground biomass across alpine grasslands, Tibetan Plateau. *Ecol. Indic.* 60 (60), 1070–1076.
- Sun, J., Wang, H.M., 2016b. Soil nitrogen and carbon determine the trade-off of the above- and below-ground biomass across alpine grasslands, Tibetan Plateau. *Ecol. Indic.* 60, 1070–1076.
- Sun, J., Cheng, G., Li, W., Sha, Y., Yang, Y., 2013a. On the variation of NDVI with the principal climatic elements in the Tibetan Plateau. *Remote Sens.* 5 (4), 1894–1911.
- Sun, J., Cheng, G.W., Li, W.P., 2013b. Meta-analysis of relationships between environmental factors and aboveground biomass in the alpine grassland on the Tibetan Plateau. *Biogeosciences* 10 (3), 1707–1715.
- Sun, J., et al., 2014. Effects of grazing regimes on plant traits and soil nutrients in an alpine steppe, Northern Tibetan Plateau. *PLoS One* 9 (9).
- Sun, J., Qin, X., Yang, J., 2016a. The response of vegetation dynamics of the different alpine grassland types to temperature and precipitation on the Tibetan Plateau. *Environ. Monit. Assess.* 188 (1), 1–11.
- Sun, J., Qin, X.J., Yang, J., 2016b. The response of vegetation dynamics of the different alpine grassland types to temperature and precipitation on the Tibetan Plateau. *Environ. Monit. Assess.* 188 (1).
- Sun, L., et al., 2017. Leaf elemental stoichiometry of *Tamarix* Lour. species in relation to geographic, climatic, soil, and genetic components in China. *Ecol. Eng.* 106, 448–457.
- Sun, J., Ma, B., Lu, X., 2018. Grazing enhances soil nutrient effects: trade-offs between aboveground and belowground biomass in alpine grasslands of the Tibetan Plateau. *Land Degrad. Dev.* 29 (2), 337–348.
- Szeicz, G., 1974. Solar radiation for plant growth. *J. Appl. Ecol.* 11 (2), 617–636.
- Takashima, T., Hikosaka, K.T., 2010. Photosynthesis or persistence: nitrogen allocation in leaves of evergreen and deciduous *Quercus* species. *Plant Cell Environ.* 27 (8), 1047–1054.
- Vanni, M.J., Flecker, A.S., Hood, J.M., Headworth, J.L., 2002. Stoichiometry of nutrient recycling by vertebrates in a tropical stream: linking species identity and ecosystem processes. *Ecol. Lett.* 5 (2), 285–293.
- Vargo, L.J., Galewsky, J., Rupper, S., Ward, D.J., 2018. Sensitivity of glaciation in the arid subtropical Andes to changes in temperature, precipitation, and solar radiation. *Global Planet. Change.*
- Wang, G., Wang, Y., Li, Y., Cheng, H., 2007. Influences of alpine ecosystem responses to climatic change on soil properties on the Qinghai-Tibet plateau, China. *Catena* 70 (3), 506–514.
- Wang, L., et al., 2015. C:N:P stoichiometry and leaf traits of halophytes in an arid saline environment, Northwest China. *PLoS One* 10 (3), e0119935.
- Wiegand, C.L., Namken, L.N., 1966. Influences of plant moisture stress, solar radiation, and air temperature on Cotton leaf temperature 1. *Agron. J.* 58 (6), 582–586.
- Wu, T.G., Yu, M.K., Wang, G.G., Dong, Y., Cheng, X.R., 2012. Leaf nitrogen and phosphorus stoichiometry across forty-two woody species in Southeast China. *Biochem. Syst. Ecol.* 44 (10), 255–263.
- Wu, T., et al., 2014. Patterns of leaf nitrogen and phosphorus stoichiometry among *Quercus acutissima* provenances across China. *Ecol. Complex.* 17 (1), 32–39.
- Xing, Z.P., et al., 2017. Temperature and solar radiation utilization of rice for yield formation with different mechanized planting methods in the lower reaches of the Yangtze River, China. *J. Integr. Agric.* 16 (9), 1923–1935.
- Xu, D., Zhang, D., Zhang, R., 1992. Photoinhibition of photosynthesis in plants. *Plant Physiol. Commun.* 4, 237–243.
- Zeng, Y., Qiu, X., Pan, A., Liu, C., 2008. Distributed modeling of global solar radiation over rugged terrain of the yellow River Basin. *Adv. Earth Sci.* 23 (11), 1185–1193.
- Zhang, M., et al., 2009. Effects of solar radiation on net ecosystem exchange of broad-leaved-Korean pine mixed forest in Changbai Mountain, China. *Chin. J. Plant Ecol.* 33 (2), 270–282.
- Zheng, Y., et al., 2012a. Winter wheat photosynthesis and dry matter production under decreased solar irradiance: a simulation study. *Chin. J. Ecol.* 31 (3), 583–593.
- Zheng, Y.F., Li, P., Wu, F.F., Wu, R.J., Yao, J., 2012b. Effects of reduced solar irradiance and enhanced O₃ on phosphorus concentration, distribution and translocation of winter wheat plant. *Chin. J. Agrometeorol.* 33 (3), 402–411.
- Zhuo, G., 2017. Spatio-temporal variation of vegetation coverage over the Tibetan Plateau and its responses to climatic factors. *Acta Ecol. Sin.* 38 (9), 2–11.